63-3-5

405888

405888

NWL Report No. 1854

ACOUSTIC RAYS IN AN OCEAN WITH HEAT SOURCE OR THERMAL MIXING ZONE

by

Hans J. Lugt and Peter Ugincius
Computation and Analysis Laboratory

U. S. NAVAL WEAPONS LABORATORY
DAHLGREN, VIRGINIA

U. S. Naval Weapons Laboratory
Dahlgren, Virginia

Acoustic Rays in an Ocean

With Heat Source or Thermal Mixing Zone

by

Hans J. Lugt and Peter Ugincius
Computation and Analysis Laboratory

NWL Report No. 1854

Task Assignment
No. R360FR103/2101/R01101001

March, 1963

TABLE OF CONTENTS

ABSTRACT

The eikonal equation of ray acoustics is discussed for the general case, with the index of refraction a function of the three space coordinates. Two examples illustrating the influences of a two-dimensional heat source and a thermal mixing zone on the acoustic ray paths are presented. Numerical results show that for long range acoustical ray tracing inhomogeneities of the ocean in the horizontal plane can cause refraction effects, which are not negligible in comparison with effects in the vertical direction. Rays, which travel in the vicinity of a heat source, can be refracted as much as 6°. Thermal mixing zones can increase the range of shadow zones near the ocean surface up to 50%. Even new shadow zones can be formed.

FOREWORD

This work was sponsored by the Naval Weapons Laboratory Foundational Research Program. It was performed in the Computation and Analysis Laboratory as part of the Meteorological and Oceanographical project (R360FR103/2101/R01101001).

The date of completion was 29 March, 1963.

Approved for Release:

/s/ R. H. LYDDANE
Technical Director

1. Introduction

In oceanography ray acoustics is usually applied to media in which the speed of sound changes only in one direction. [1], [2]. This restriction is justified for most practical purposes because variations of the speed of sound are much larger in the vertical direction of the ocean than in the horizontal plane. Better knowledge of the ocean currents in recent years raises the question about the influence of a general three-dimensional gradient of the speed of sound on long-range acoustical ray tracing.

For this reason the Naval Weapons Laboratory has prepared a program for the solution of the eikonal equation in which the speed of sound can be a general function of the space coordinates. This program will be used in the near future to solve special practical problems.

In this study the basic equations are discussed, and the coded program is applied on two models representing a heat source and a thermal mixing zone in the ocean. These models are rather artificial because the detailed features of oceanic inhomogeneities are complex and transient. They serve, however, to demonstrate the magnitude of refraction one may expect in the oceans under such conditions. The influence of small-scale fluctuations has not been considered.

2. Basic Assumptions and Equations

All ocean currents are very slow compared with the speed of sound so that their velocities can be neglected. They are, however, often

connected with large gradients of temperature and salinity, which influence the speed of sound. The medium in consideration, therefore, can be regarded as isotropic but inhomogeneous. Presuming, furthermore, the validity of ray acoustics — that the speed of sound does not change much in distances of the order of one wave length — one can use the eikonal equation (see e. g. Chernov [3]):

$$\frac{d}{ds}\left(n\,\frac{d\vec{r}}{ds}\right) = \nabla n \tag{1}$$

where s = arc length along the ray path from a given starting point

$\vec{r} = \vec{r}(s)$ the position vector of the ray

n = index of refraction of the medium

In a cartesian coordinate system (x, y, z) equation (1) is equivalent to the following three ordinary differential equations of second order:

$$\ddot{x} + \frac{1}{n}\frac{\partial n}{\partial x}\dot{x}^2 + \frac{1}{n}\frac{\partial n}{\partial y}\dot{x}\dot{y} + \frac{1}{n}\frac{\partial n}{\partial z}\dot{x}\dot{z} = \frac{1}{n}\frac{\partial n}{\partial x} \tag{2}$$

$$\ddot{y} + \frac{1}{n}\frac{\partial n}{\partial x}\dot{y}\dot{x} + \frac{1}{n}\frac{\partial n}{\partial y}\dot{y}^2 + \frac{1}{n}\frac{\partial n}{\partial z}\dot{y}\dot{z} = \frac{1}{n}\frac{\partial n}{\partial y} \tag{3}$$

$$\ddot{z} + \frac{1}{n}\frac{\partial n}{\partial x}\dot{z}\dot{x} + \frac{1}{n}\frac{\partial n}{\partial y}\dot{z}\dot{y} + \frac{1}{n}\frac{\partial n}{\partial z}\dot{z}^2 = \frac{1}{n}\frac{\partial n}{\partial z} \tag{4}$$

where the dots denote the derivatives with respect to s. The ray path is determined by the initial conditions

$$s = s_0: \quad x_0,\ y_0,\ z_0; \quad \dot{x}_0,\ \dot{y}_0,\ \dot{z}_0. \tag{5}$$

The set of equations (2) through (4) is programmed for solution by the Runge-Kutta method on the computer IBM - 7090.

By elimination of the implicit parameter s equations (2) through (4) may be combined into two equations:

$$y'' + (1 + y'^2 + z'^2)\left(\frac{1}{n}\frac{\partial n}{\partial x}y' - \frac{1}{n}\frac{\partial n}{\partial y}\right) = 0 \tag{6}$$

$$z'' + (1 + y'^2 + z'^2)\left(\frac{1}{n}\frac{\partial n}{\partial x}z' - \frac{1}{n}\frac{\partial n}{\partial z}\right) = 0 \tag{7}$$

The primes here indicate differentiation with respect to x. The initial conditions (5) become

$$x = x_0: \quad y_0,\ z_0;\quad y_0',\ z_0'. \tag{8}$$

The index of refraction is a function of the temperature T, the salinity S, and the pressure p of the medium:

$$n = n(T, S, p) \tag{9}$$

with

$$T = T(x, y, z) \tag{10}$$

$$S = S(x, y, z) \tag{11}$$

$$p = p(z) \tag{12}$$

if the coordinate z is chosen normal to the ocean surface. For the calculation of the index of refraction (9) as a function of T, S, and p the formula by Wilson [4] has been used. The functions (10) and (11)

depend on the medium under consideration. p(z) is given by the hydrostatic equation. From (9) through (12) there follows

$$n = n(x, y, z) \tag{13}$$

Equations (6) and (7) are in general too complicated to yield an analytic solution if the index of refraction is a function of more than one variable. Only in special cases are analytic solutions possible. Two such cases are briefly examined for $n = n(x, y)$ in the next section.

3. Discussion of the Eikonal Equation for the Two-dimensional Case

A medium will be assumed in which the index of refraction is only a function of the coordinates x and y, i. e. $\frac{\partial n}{\partial z} = 0$. In addition only those rays will be considered which start out initially in the (x, y) plane. Then, because of the restriction $\frac{\partial n}{\partial z} = 0$ they will remain in that plane. The differential equations (6) and (7) reduce to

$$y'' + (1 + y'^2)\left(\frac{1}{n}\frac{\partial n}{\partial x}y' - \frac{1}{n}\frac{\partial n}{\partial y}\right) = 0 \tag{14}$$

with the initial conditions

$$x = x_0: \qquad y_0, \; y_0' \; . \tag{15}$$

In general, the differential equation (14) cannot be solved in a closed form. There exist, however, classes of analytic solutions

which will be discussed briefly.

A first integral can be obtained if the last factor in equation (14) represents an exact differential $d\Psi$:

$$\frac{1}{n}\frac{\partial n}{\partial x}\,dy - \frac{1}{n}\frac{\partial n}{\partial y}\,dx = d\Psi \tag{16}$$

According to Kamke [5], the first integral is

$$y' = -\tan(\Psi + \text{const.}) \tag{17}$$

Equation (16) holds if the function n satisfies the condition

$$n\nabla^2 n = |\nabla n|^2 \tag{18}$$

or:
$$n = \phi_1(x + iy)\phi_2(x - iy) \tag{19}$$

where only real values of n are of interest. ϕ_1 and ϕ_2 are arbitrary functions of the complex number $x + iy$ and its conjugate $x - iy$. In many practical cases the approximation

$$\frac{1}{n}\frac{\partial n}{\partial x} \approx \frac{\partial n}{\partial x} \tag{20}$$

may be used. The condition (18), then, is replaced by the Laplace equation $\nabla^2 n = 0$ with the well-known general solution
$n = \varphi_1(x + iy) + \varphi_2(x - iy)$.

Another class of analytic solutions of equation (14) can be found by choosing

$$\frac{\partial n}{\partial x} y' - \frac{\partial n}{\partial y} = 0 \qquad (21)$$

The ray paths are straight lines because $y'' = 0$. Besides the trivial case $n = \text{const}$, which is also a solution of (18), equation (21) will be satisfied if

$$\frac{\partial n}{\partial y} = K \frac{\partial n}{\partial x} ; \qquad y' = K = \text{const.} \qquad (22)$$

The solution of equation (22) is:

$$n = n(x + Ky) \qquad (23)$$

Thus, in a medium described by the above index of refraction, one ray (with the initial slope K) will be propagated as a straight line.

4. Two-dimensional Heat Source in an Infinite Ocean

The ray paths near a heat source will be calculated numerically by considering only paths in the horizontal plane (x, y). In practice a heat source may be represented by a melting iceberg or by a separated vortex flow with a temperature gradient, as it occurs in and near the Gulf Stream. The heat transfer is approximately described by the transient-state law

$$\frac{T - T_\infty}{T_0 - T_\infty} = e^{-\alpha r^2} \qquad (24)$$

where $r^2 = x^2 + y^2$. The heat source is located at the origin r = 0. T is the temperature in the plane (x, y), T_o the temperature at the origin, and T_∞ the temperature at infinity. The coefficient α is inversely proportional to the time. For ray tracing the dependency on the time can be neglected since the time-dependent heat transfer is small with respect to the speed of sound. Using a linear approximation for the speed of sound as a function of the temperature one obtains

$$n = 1 + ke^{-\alpha r^2} \tag{25}$$

where k is a constant proportional to the temperature difference between the heat source and the ocean at a large distance from the heat source.

Equation (14) yields with equation (25):

$$y'' + (1 + y'^2)\frac{2\alpha k(y - xy')}{k + e^{\alpha(x^2 + y^2)}} = 0 \tag{26}$$

Substituting

$$\xi = \sqrt{\alpha}\, x; \quad \eta = \sqrt{\alpha}\, y \tag{27}$$

one arrives at the normalized equation

$$\eta'' + 2k(1 + \eta'^2)\frac{\eta - \xi\eta'}{k + e^{(\xi^2 + \eta^2)}} = 0 \tag{28}$$

where the primes denote here the derivatives with respect to ξ .

Numerical solutions by means of the IBM-7090 computer are shown in Figures 1 through 4 for the following parameters

$k_1 = -0.03155$; $(T_0 = 10°C, T_\infty = 0°C)$
$k_2 = -0.06310$; $(T_0 = 20°C, T_\infty = 0°C)$
} heat source

$k_3 = +0.03155$; $(T_0 = 10°C, T_\infty = 20°C)$
$k_4 = +0.06310$; $(T_0 = 0°C, T_\infty = 20°C)$
} heat sink

For the calculation of k a linear approximation of Wilson's formula [4] has been applied.

The curves in Figures 1 through 4 can be used to construct the ray paths from a point source of sound. Two examples are shown in Figures 5 and 6, which are drawn with the aid of Figures 2 and 4, respectively.

Discussion of the results.

The divergence of ray paths is a measure of the intensity of sound waves. It can be seen that a heat source causes the bundles to diverge and thus diminishes the intensity whereas a heat sink has the opposite effect. Besides this qualitative statement the total deviation of the ray paths can be found. Figure 7 shows the total angle of deviation $\Delta\theta$ as a function of $\eta(-\infty)$ — the perpendicular distance between the asymptote of the ray and the heat source — for $T_0 - T_\infty = 20°C$. The solid curve is obtained from

the numerical solutions, and the dashed curve is the graph of the function

$$\Delta\theta = 2\sqrt{\pi}\, k\, \eta(-\infty) e^{-[\eta(-\infty)]^2} \tag{29}$$

Equation (29) is derived in Appendix A as a first order approximation without knowing the actual ray paths. The agreement of the two curves is satisfactory.

From Figure 7 it is seen that rays passing near a heat source can be refracted up to 6°. This may be regarded as a measure for the magnitude of error that can occur if a change of the refraction index in the horizontal direction of an ocean with a heat source is not considered.

5. Thermal Mixing Zone in an Ocean

In this example ray tracing in the vertical cross-section of the boundary layer between two fluid flows normal to the flow directions is examined. The flows have different temperatures so that a thermal mixing zone associated with the momentum boundary layer exists.

Let the cross-section be the (y, z) plane which is normal to the flow direction x. The horizontal temperature distribution at the ocean surface z = 0 in the y-direction is assumed to be proportional to the flow velocity and according to Schlichting [6] :

$$\frac{T(y,0) - T(-\infty,0)}{T(\infty,0) - T(-\infty,0)} = \operatorname{erf}(y - \bar{y}) = \frac{1}{\sqrt{\pi}} \int_{-\infty}^{y-\bar{y}} e^{-t^2} dt \tag{30}$$

where $T(-\infty, 0)$ and $T(\infty, 0)$ are the surface temperatures of the colder fluid and the warmer fluid, respectively, and $\bar{y}$ is the point of inflection of $T(y, 0)$. For the vertical temperature distribution of the colder fluid an empirical function $h(z)$ is used, which is typical for the ocean (see Fig. 8)[2]:

$$h(z) = \frac{T(-\infty, z) - T(-\infty, 0)}{T(-\infty, 0) - T(-\infty, z_B)} \tag{31}$$

where $T(-\infty, z_B)$ is the temperature of the colder fluid at the bottom.

The function $h(z)$ is obtained by linear interpolation of the temperature vs. depth graph in Figure 8. The points between which this interpolation is made are tabulated in Appendix B. The temperature is constant for $0 \leq z \leq 60$. The main thermocline extends from $z = 60$ to about 1500 m. For depths greater than 3000 m, the temperature is constant again. Figure 8 also shows the speed of sound V vs. depth for the colder fluid ($y = -\infty$). It will be observed that V has a relative maximum at $z = 60$ m. The minimum occurs at $z = 600$ m, which is the depth of the deep sound channel.

In order to obtain the temperature distribution over the entire (y, z) plane it is assumed that for any line $z = \text{const}$ the temperature distribution is similar to that for $z = 0$ and that the difference $T(-\infty, z) - T(+\infty, z)$ varies in the same way as $h(z)$. The complete temperature distribution in the (y, z) plane can then be

expressed by

$$T(y, z) = T(-\infty, 0) + [T(-\infty, 0) - T(-\infty, z_B)]h(z) + [T(\infty, \upsilon) - T(-\infty, 0)][1 + h(z)]\mathrm{erf}(y - \bar{y}) \quad . \quad (32)$$

Assumption (32) implies that the velocity of the flow as a function of the depth is proportional to the vertical temperature distribution. This hypothesis, although not borne out conclusively, is at least not contradicted by available experimental results. See Stommel [7] .

The surface of the ocean is taken as a specular reflector, and the bottom is assumed to be a perfect absorber.

For numerical calculations the following data are chosen which represent typical values for the Gulf Stream:

$T(-\infty, 0) = 12°C$, $\qquad T(+\infty, 0) = 27°C$

$T(-\infty, z_B) = 2°C$

$z_B = 5000$ m

$S = 35\ {}^{o}/_{oo}$

$p = (1.033 + 0.1023z)\mathrm{kg\ cm}^{-2}$

The computed ray paths are shown in figures 9 through 17. Each ray is identified by the angle it makes initially with the ocean surface. The sound source is located at three different depths: z = 0, 600 and 3000 m for each of two positions inside

the thermal mixing zone: at y = 0, and y = 30 km. The latter position corresponds to the inflection point $\overline{y}$ of the error function (30). The scale of y is then determined by letting the distance between y = 0 and y = 30 km correspond to three standard deviations of the error function (30). Computations were carried out up to a range of 100 km.

Discussion of the Results

Figures 9 through 11 show ray paths in an ocean in which the speed of sound varies only with depth as in Figure 8.

With the sound source at the surface (Figure 9) all rays with an angle of inclination $\theta_0 < 2°5'$ are confined in a shallow layer 60 m below the surface. Rays with $2°5' \leq \theta_0 \leq 13°55'$ are bent downwards till they reach the depth of the sound channel (600 m), and then are bent upwards again. This results in a large shadow zone extending up to a range of 47 km - region A. Rays with $\theta_0 > 13°55'$ are absorbed by the bottom, so that two other shadow zones — regions B and C — are formed. If the bottom were removed ($z_B = \infty$) these shadow zones would not exist, but one can easily see that the intensity would be relatively low.

In Figure 10 the sound source is placed at the deep sound channel depth (z = 600 m). The rays oscillate about this channel, which is a well known result [2], [8]. Three shadow zones are formed: regions A, B, and C. In contrast to Figure 9 the regions

A and B extend up to the surface.

In Figure 11 the sound source is located 3000 m below the surface, at the depth where the vertical change of the temperature becomes zero. All rays with $\theta_0 \leq 12°$ are bent up to and reflected by the surface, those with $\theta_0 > 12°$ are absorbed by the bottom, causing the formation of two shadow zones: regions A and B.

Figures 12 through 14 show the ray paths in an ocean with the two-dimensional temperature distribution (32), and are directly comparable with the preceding Figures 9 through 11. In general it can be noted that the effect of the thermal mixing zone is to depress the rays downwards, and thus to enhance all surface shadow zones, and even create some new ones.

A comparison of Figures 9 and 12 shows that the shadow zone A now extends up to a range of 60 km instead of 47 km — an increase of 29%.

The influence of the thermal mixing zone has created another interesting effect, which is not shown in Figure 12. Because the rays are gradually shifted downwards, all of the rays with $\theta_0 < 2°5'$ are not confined any more within the shallow 60 m surface layer as in Figure 9. Every time the limiting ray in this surface layer reaches its nadir, a small packet of rays will have been shifted downwards far enough so that it penetrates the 60 m depth and is subjected to the negative speed of sound gradient of the

main thermocline. To show this effect the ray paths for five such rays have been calculated and are plotted in Figure 18. One sees that the regions A, B, and C in Figure 12 are not real shadow zones, but are interlaced with these narrow bundles of rays. It must be observed that this effect would not appear if the speed of sound vs. depth profile had a continuous first derivative at z = 60 m.

In Figure 13 the deep sound channel with the oscillating rays slopes downwards with increasing range. The shadow zones A and B are substantially enlarged as compared with the corresponding shadow zones in Figure 10. The range of A has increased by 43%.

Figure 14 shows that the thermal mixing zone has formed two new shadow zones near the surface — regions C and D — which are not present in Figure 11.

Figures 15 through 17 show the corresponding ray paths with the sound source placed at the point of inflection of the thermal mixing zone (y = 30 km). Here it will be noticed that the depression of the rays is even more pronounced than in Figures 12-14, because now the source is at the position where the effect of the mixing zone is the greatest. Comparison of Figures 16 and 10 shows an increase of 51% in the range of A.

In connection with the shadow zones A, B, and C in Figure 15, the same comments as for Figure 12 apply.

References

[1] L. M. BREKHOVSKIKH, Waves in Layered Media. Academic Press, Publishers, New York, London, 1960.

[2] The Physics of Sound in the Sea. NDRC Summary Technical Reports, Div. 6, Vol. 8. Washington, D. C., 1946.

[3] L. A. CHERNOV, Wave Propagation in a Random Medium. McGraw-Hill Book Co., Inc., New York, Toronto, London, 1960.

[4] W. D. WILSON, Equations for the computation of the speed of sound in sea water. NAVORD Rep. 6906, 5 July 1960.

[5] E. KAMKE, Differentialgleichungen, Lösungsmethoden und Lösungen. 3rd Ed. Chelsea, New York, 1959.

[6] H. SCHLICHTING, Boundary Layer Theory, Fourth Edition, 1960, p. 599.

[7] H. STOMMEL, The Gulf Stream, University of California Press, 1960, p. 58.

[8] C. B. OFFICER, Introduction to the Theory of Sound Transmission with Application to the Ocean, McGraw-Hill Book Co., Inc., New York, Toronto, London, 1958.

APPENDIX A

Approximate Equation for Total Angle of Deviation for a Ray Near a Heat Source

In general the curvature of a line is given by:

$$\kappa = \frac{d\theta}{ds} = \left| \frac{d^2\vec{r}}{ds^2} \right| = \sqrt{\left(\frac{d^2x}{ds^2}\right)^2 + \left(\frac{d^2y}{ds^2}\right)^2 + \left(\frac{d^2z}{ds^2}\right)^2} \quad . \tag{A-1}$$

From the eikonal equation (1) there follows:

$$\frac{d^2\vec{r}}{ds^2} = \frac{1}{n}\left(\nabla n - \frac{dn}{ds}\frac{\vec{dr}}{ds}\right) \tag{A-2}$$

From (A-2) the curvature of a sound ray becomes:

$$\kappa = \frac{1}{n}\sqrt{|\nabla n|^2 - \left(\nabla n \cdot \frac{\vec{dr}}{ds}\right)^2} \quad ,$$

or:
$$\kappa = \frac{|\nabla n|}{n}\sqrt{1 - \cos^2\psi} \tag{A-3}$$

where ψ is the angle between ∇n and $\frac{\vec{dr}}{ds}$.

Equation (25) yields:

$$\nabla n = -\, 2k\rho e^{-\rho^2}(\nabla\rho) \quad , \tag{A-4}$$

where ρ is the normalized radius $\rho^2 = \xi^2 + \eta^2$.

In this problem the direction of ∇n is given by the unit vector $\nabla\rho$ with direction cosines $\frac{\xi}{\rho}$ and $\frac{\eta}{\rho}$. The ray has the direction cosines $\frac{d\xi}{ds}$ and $\frac{d\eta}{ds}$. The angle ψ is given by:

$$\cos\psi = \frac{1}{\rho}\left(\xi\frac{d\xi}{ds} + \eta\frac{d\eta}{ds}\right) \tag{A-5}$$

The curvature (A-3) becomes

$$\kappa = \frac{d\theta}{ds} = \frac{2ke^{-\rho^2}}{1+ke^{-\rho^2}} \approx \sqrt{\rho^2 - \left(\xi \frac{d\xi}{ds} + \eta \frac{d\eta}{ds}\right)^2} \quad . \tag{A-6}$$

The total angle of deviation $\Delta\theta$ between the initial and final directions of the ray is given by the line integral

$$\Delta\theta = \int_{s=s_0}^{\infty} \kappa ds \quad . \tag{A-7}$$

The equation of the ray is not known analytically, therefore this integral is evaluated with the following approximations. Since $k << 1$, $ke^{-\rho^2}$ can be neglected in the denominator of (A-6). Also, $\frac{d\eta}{ds} << \frac{d\xi}{ds}$. Therefore the approximations $\frac{d\eta}{ds} \simeq 0$, $\eta \simeq \eta(-\infty)$, $\rho^2 \simeq \xi^2 + [\eta(-\infty)]^2$, $\frac{d\xi}{ds} \simeq 1$ and $ds \simeq d\xi$ can be used. With these approximations equation (A-7) becomes

$$\Delta\theta = 2k\eta(-\infty)e^{-[\eta(-\infty)]^2} \int_{-\infty}^{\infty} e^{-\xi^2} d\xi \quad ,$$

which reduces to equation (29) in the text:

$$\Delta\theta = 2\sqrt{\pi}\, k\, \eta(-\infty)e^{-[\eta(-\infty)]^2} \quad .$$

APPENDIX B

Typical Temperature vs. Depth Data for the Ocean

In the table below are listed the depths together with the corresponding temperatures in Figure 8, between which the linear interpolations of h(z) in equation (31) are calculated.

Depth z in meters	Temp T in °C
0	12.00
60	12.00
200	7.83
250	6.72
300	5.89
350	5.33
500	4.50
600	4.06
800	3.50
1000	3.11
1500	2.67
2000	2.28
2500	2.11
3000	2.00
5000	2.00

APPENDIX C

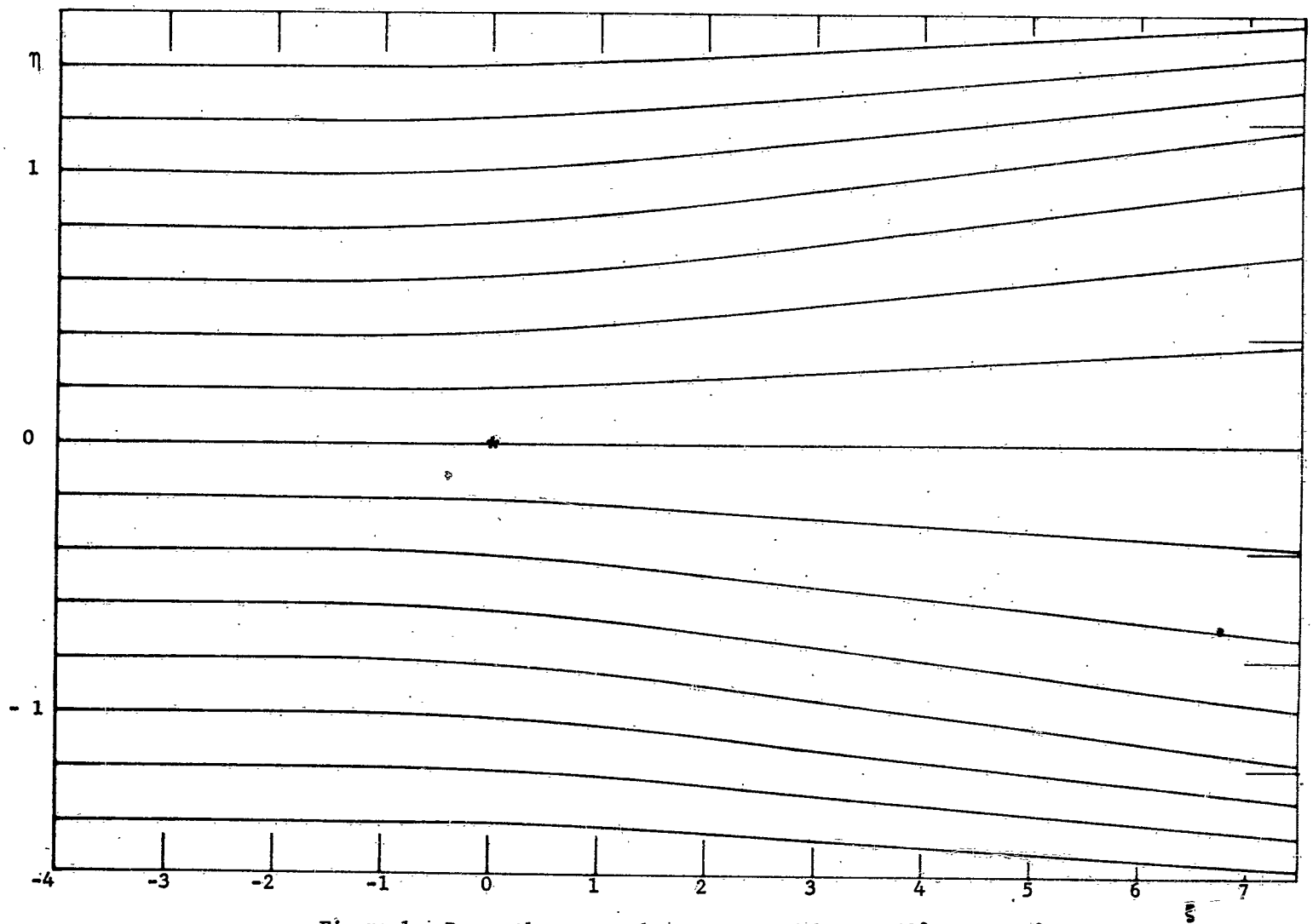

Figure 1: Ray paths near a heat source with $T_o = 10°C$, $T_\infty = 0°C$.
(* indicates position of heat source)

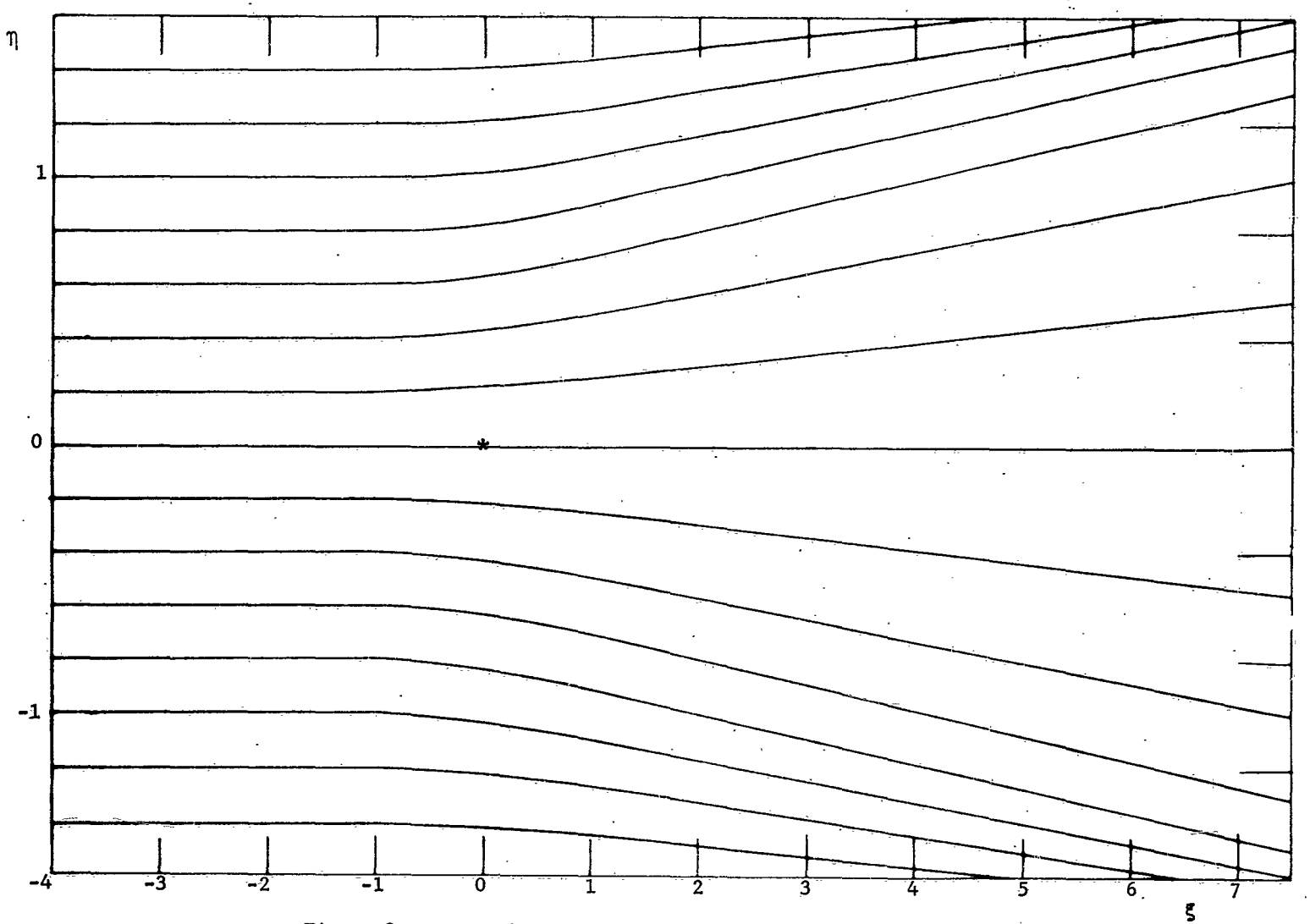

Figure 2: Ray paths near a heat source with $T_o = 20°C$, $T_\infty = 0°C$.
(* indicates position of heat source)

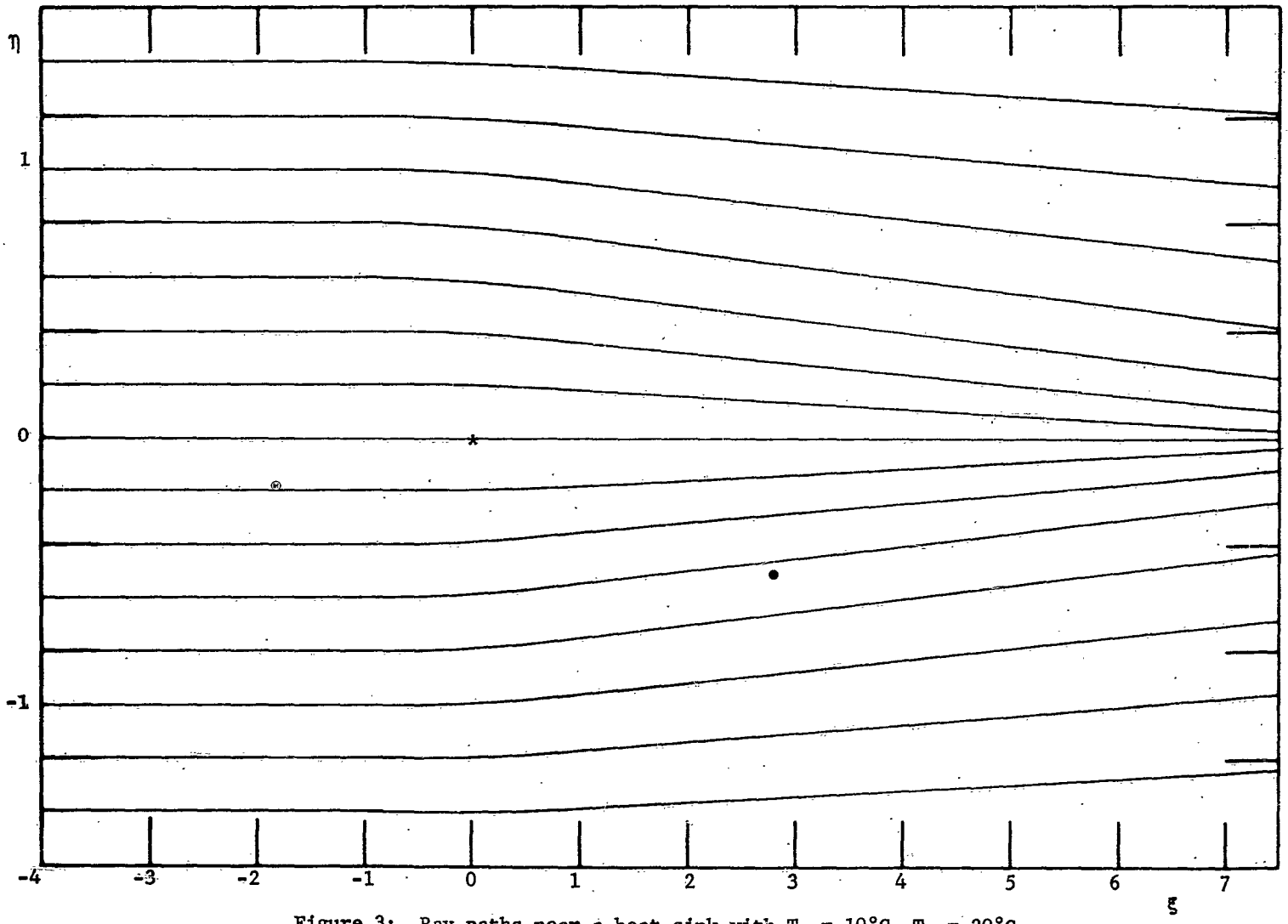

Figure 3: Ray paths near a heat sink with $T_0 = 10°C$, $T_\infty = 20°C$.
(* indicates position of heat sink)

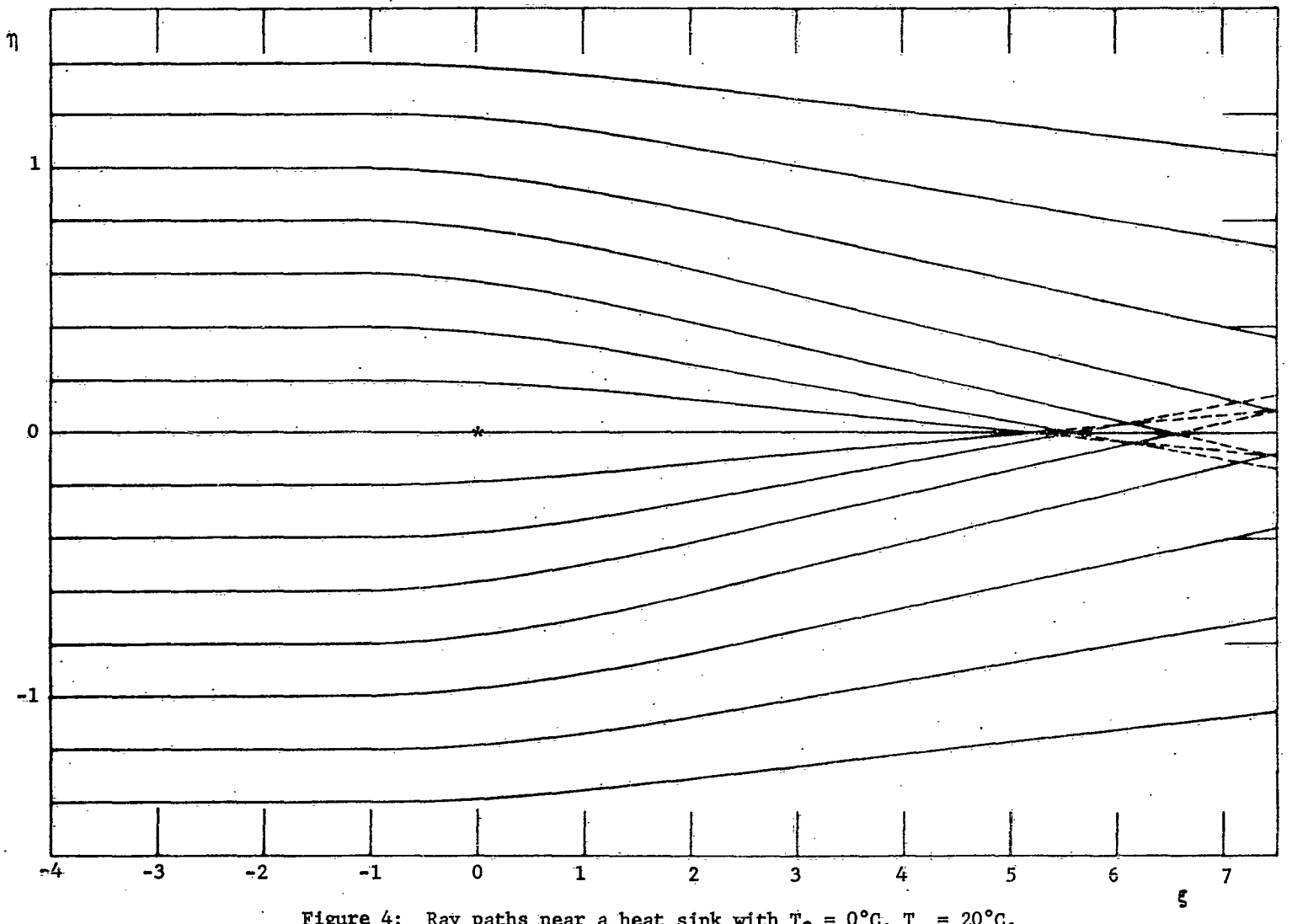

Figure 4: Ray paths near a heat sink with $T_0 = 0°C$, $T_\infty = 20°C$.
(* indicates position of heat sink)

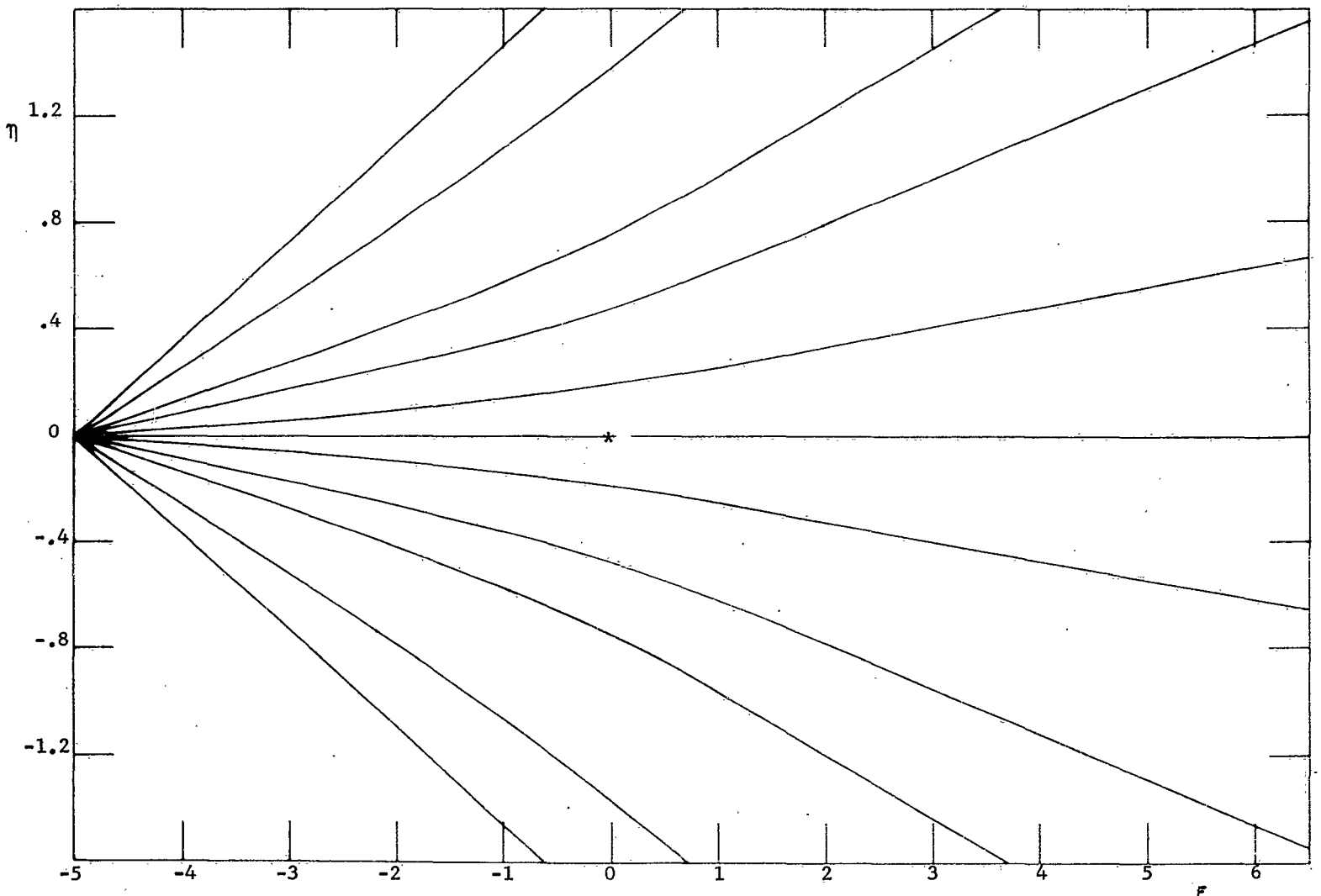

Figure 5: Ray paths from a point source of sound located at $\xi = -5$ for $T_o = 20°C$, $T_\infty = 0°C$. (* indicates position of heat source)

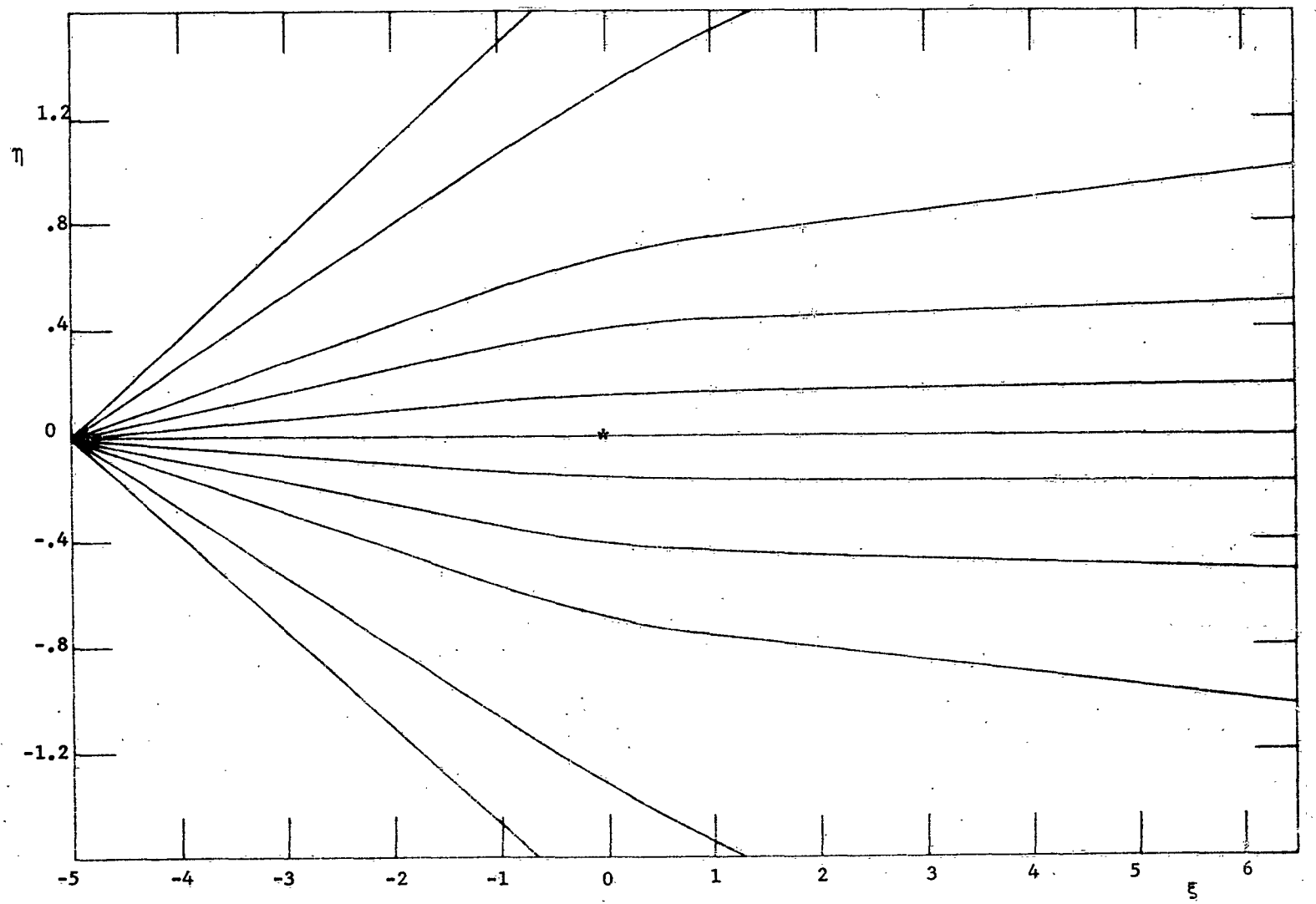

Figure 6: Ray paths from a point source of sound at $\xi = -5$ for $T_0 = 0°C$, $T_\infty = 20°C$.
(* indicates position of heat sink)

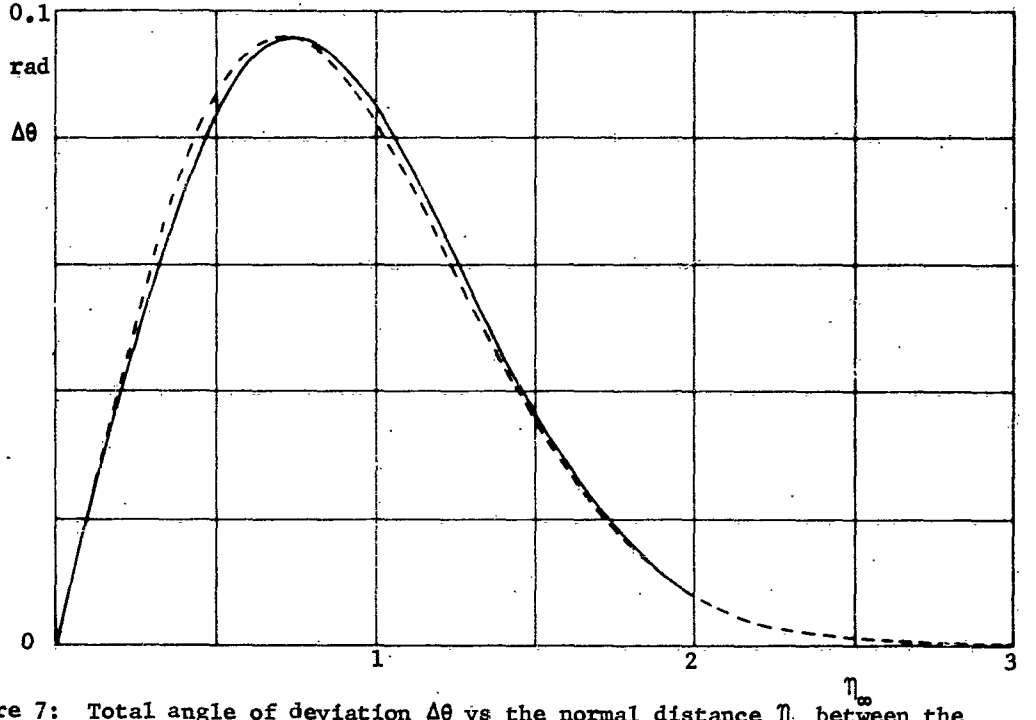

Figure 7: Total angle of deviation $\Delta\theta$ vs the normal distance η_∞ between the asymptote of the ray and the heat source for $T_0 = 20^\circ C$, $T_\infty = 0^\circ C$. The dashed curve is the graph of Equation (29).

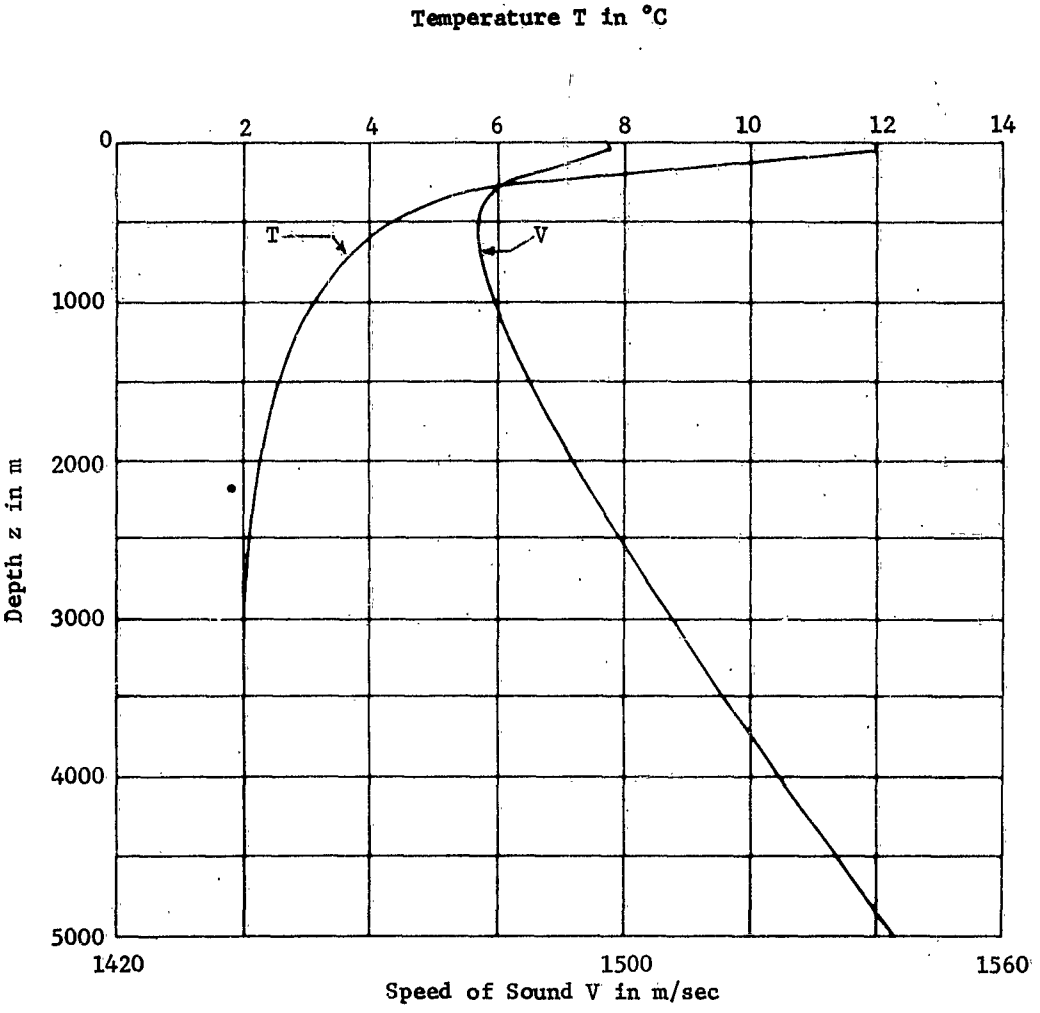

Figure 8: Temperature T and speed of sound V vs. depth z at $y = -\infty$.

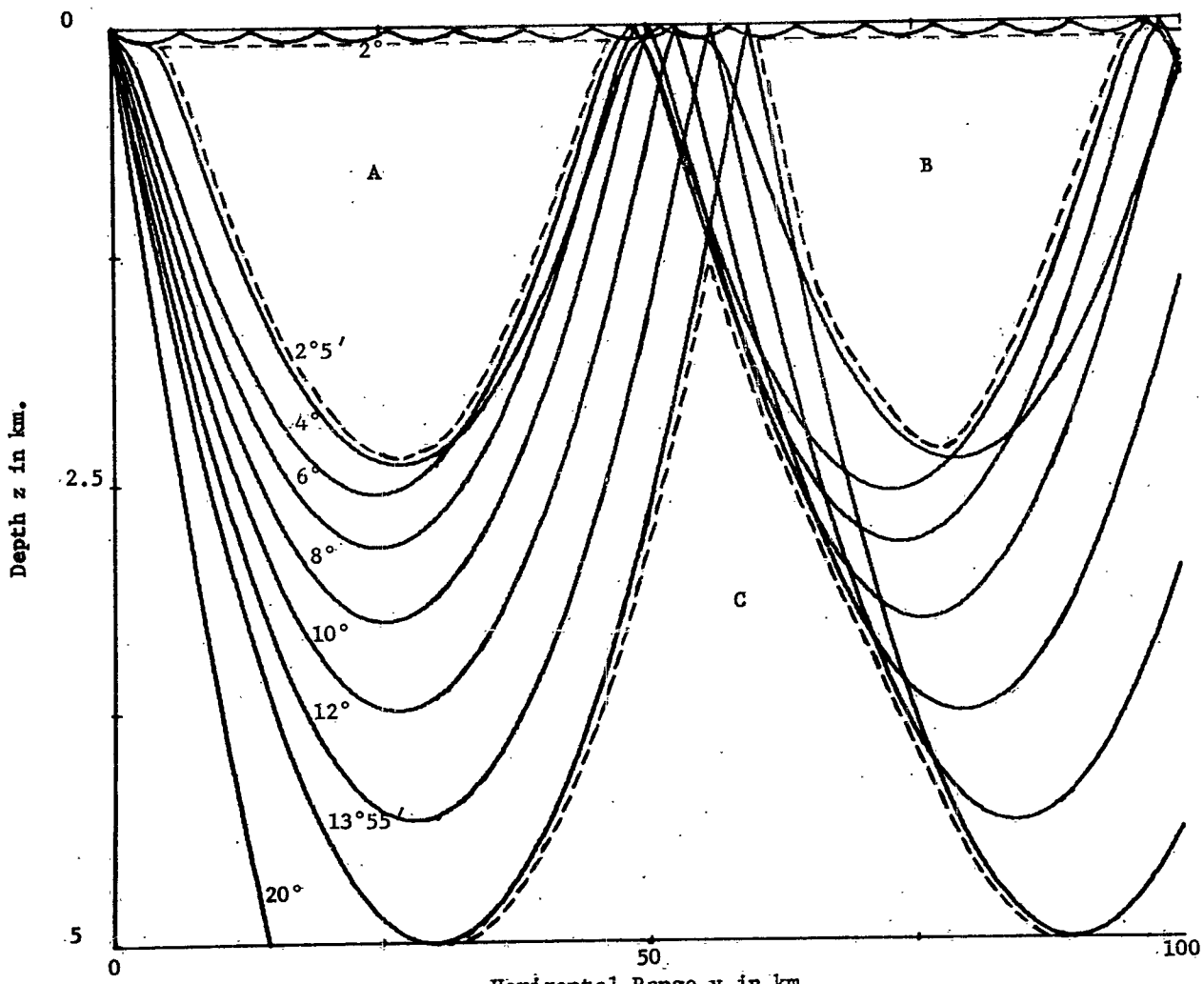

Figure 9: Ray paths in an ocean with the speed of sound a function of depth only. Sound source at z = 0 m.

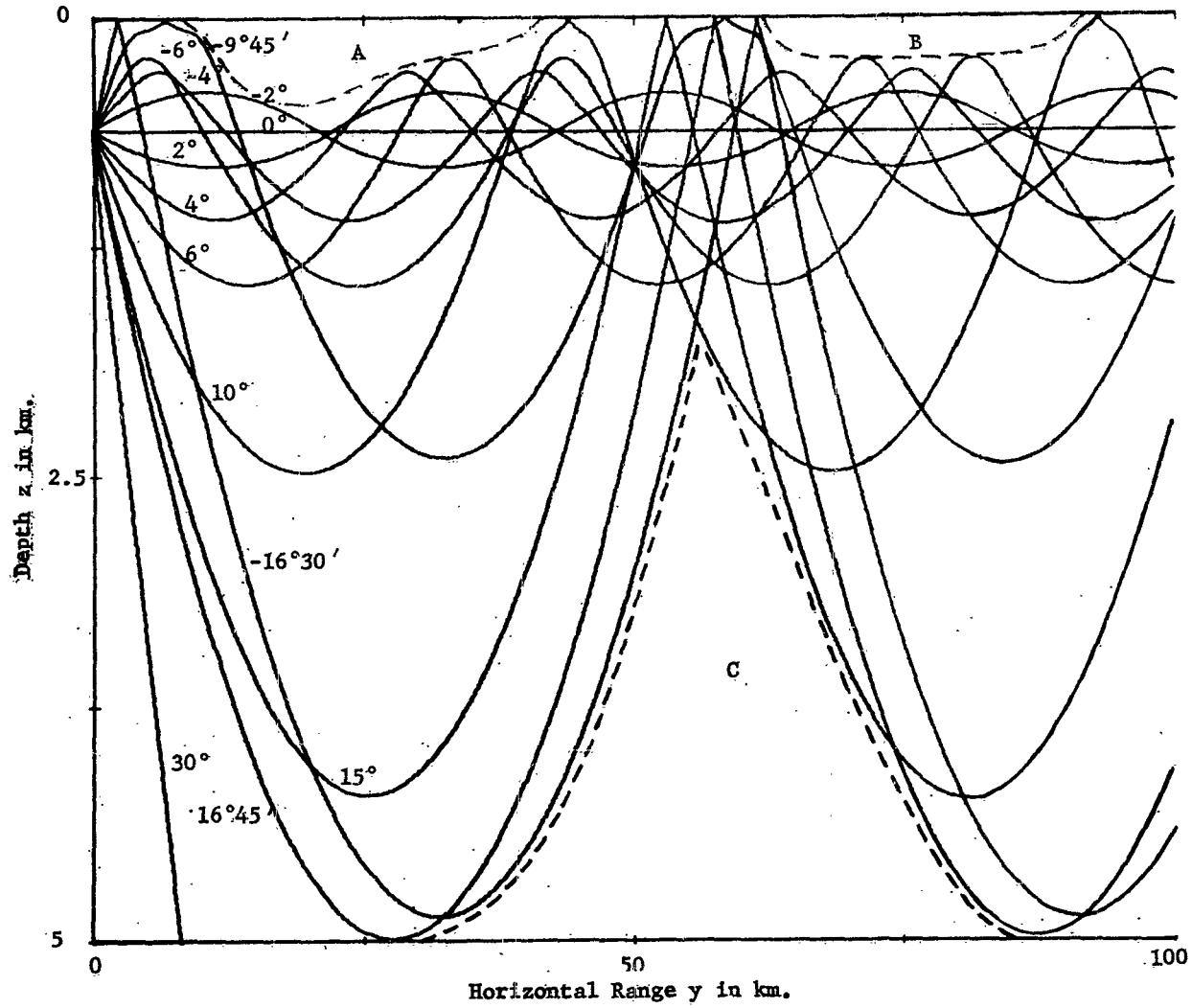

Figure 10: Ray paths in an ocean with the speed of sound a function of depth only. Sound source at z = 600 m.

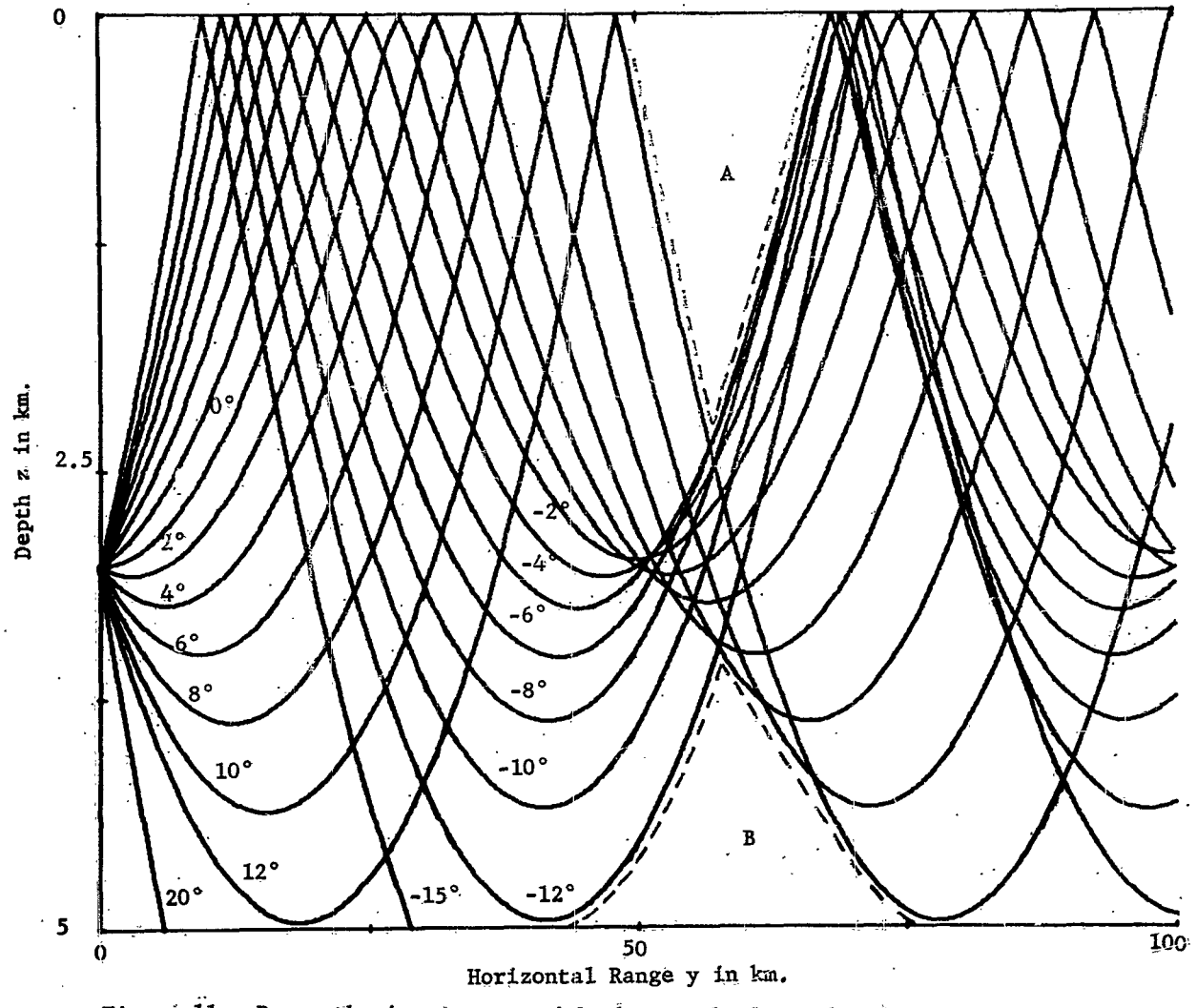

Figure 11: Ray paths in an ocean with the speed of sound a function of depth only. Sound source at z = 3000 m.

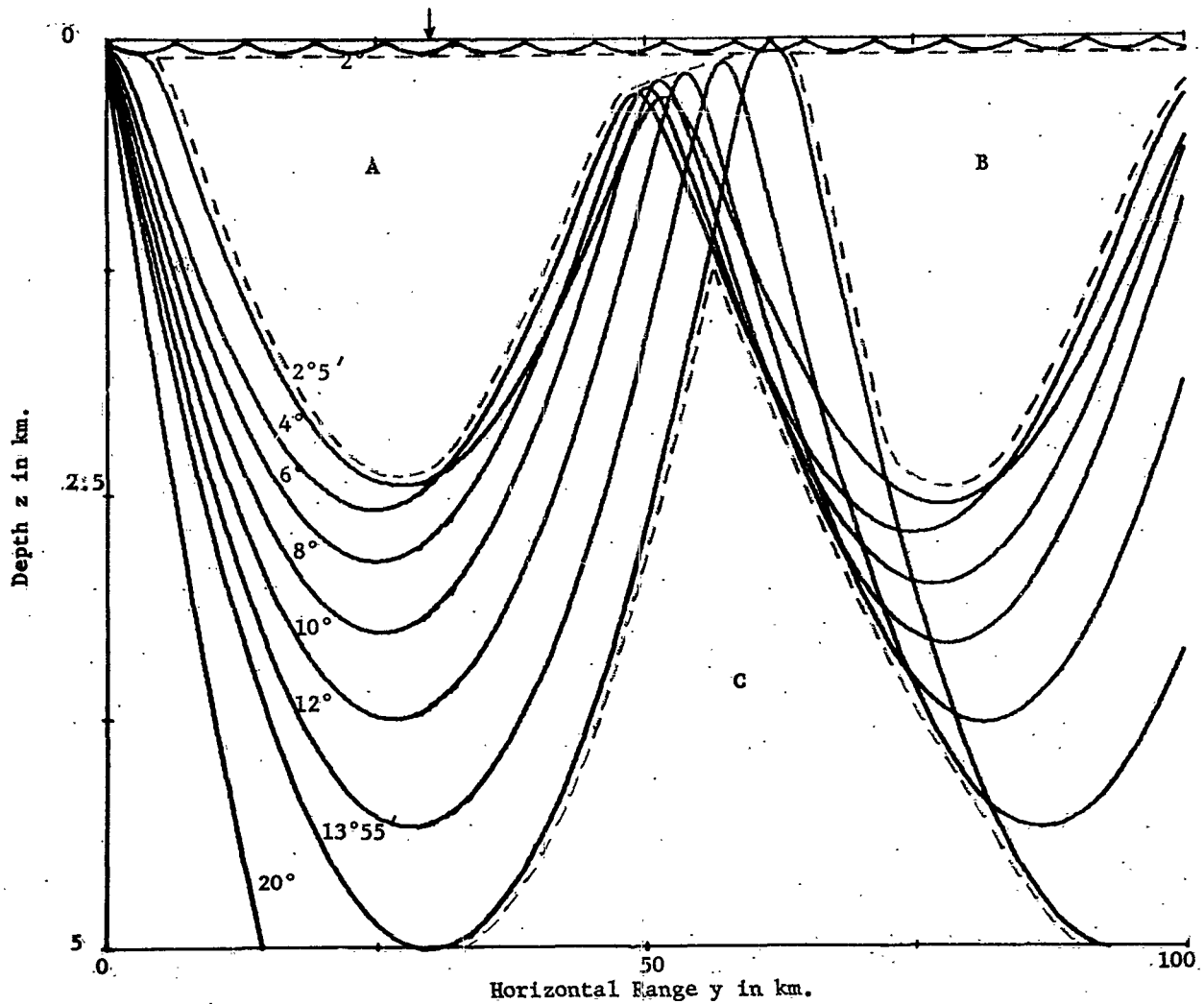

Figure 12: Ray paths in an ocean with a thermal mixing zone. Sound source at z = 0 m, y = 0 m. (Arrow indicates inflection point of the thermal mixing zone.)

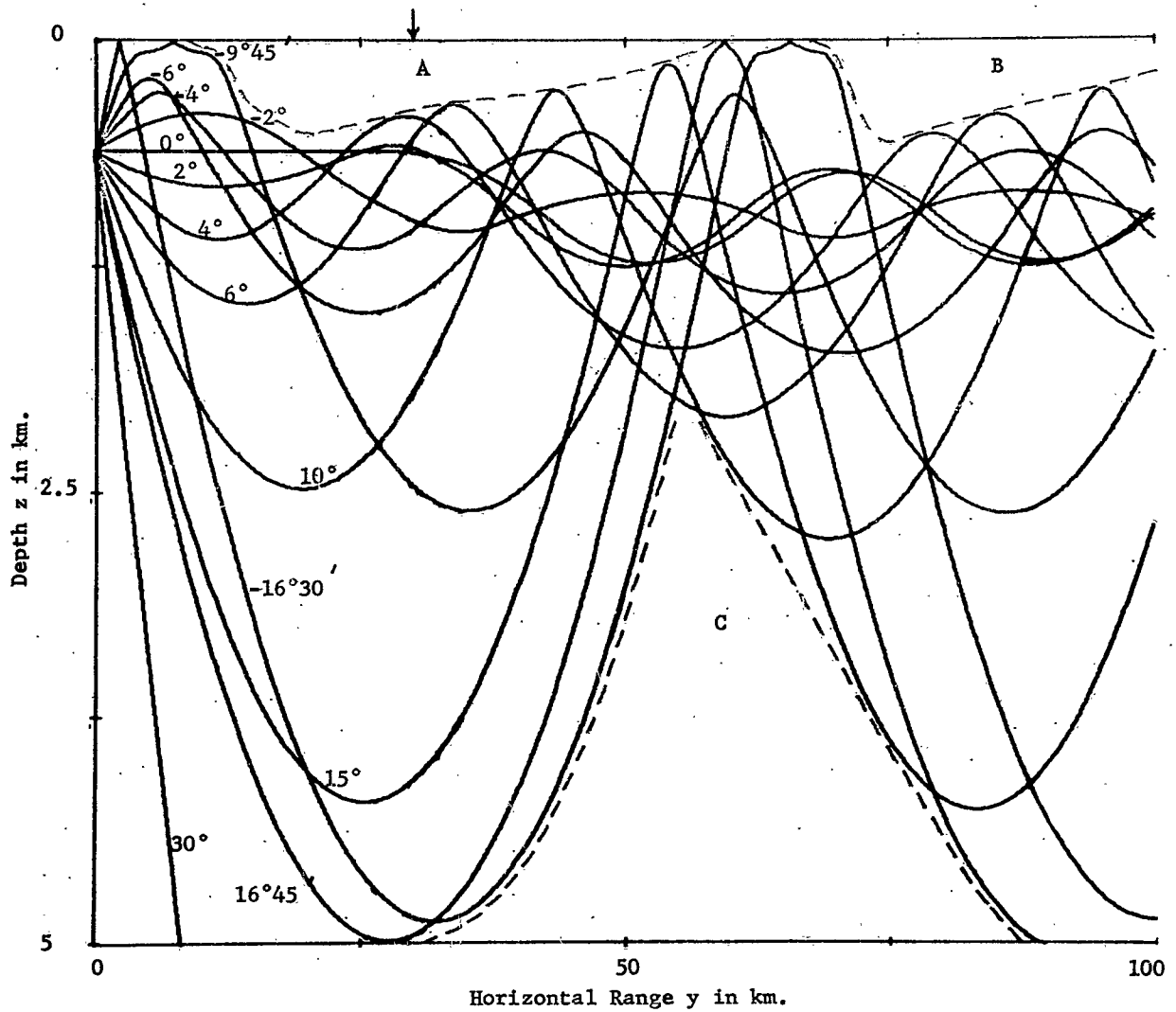

Figure 13: Ray paths in an ocean with a thermal mixing zone. Sound source at z = 600 m, y = 0 m. (Arrow indicates inflection point of the thermal mixing zone.)

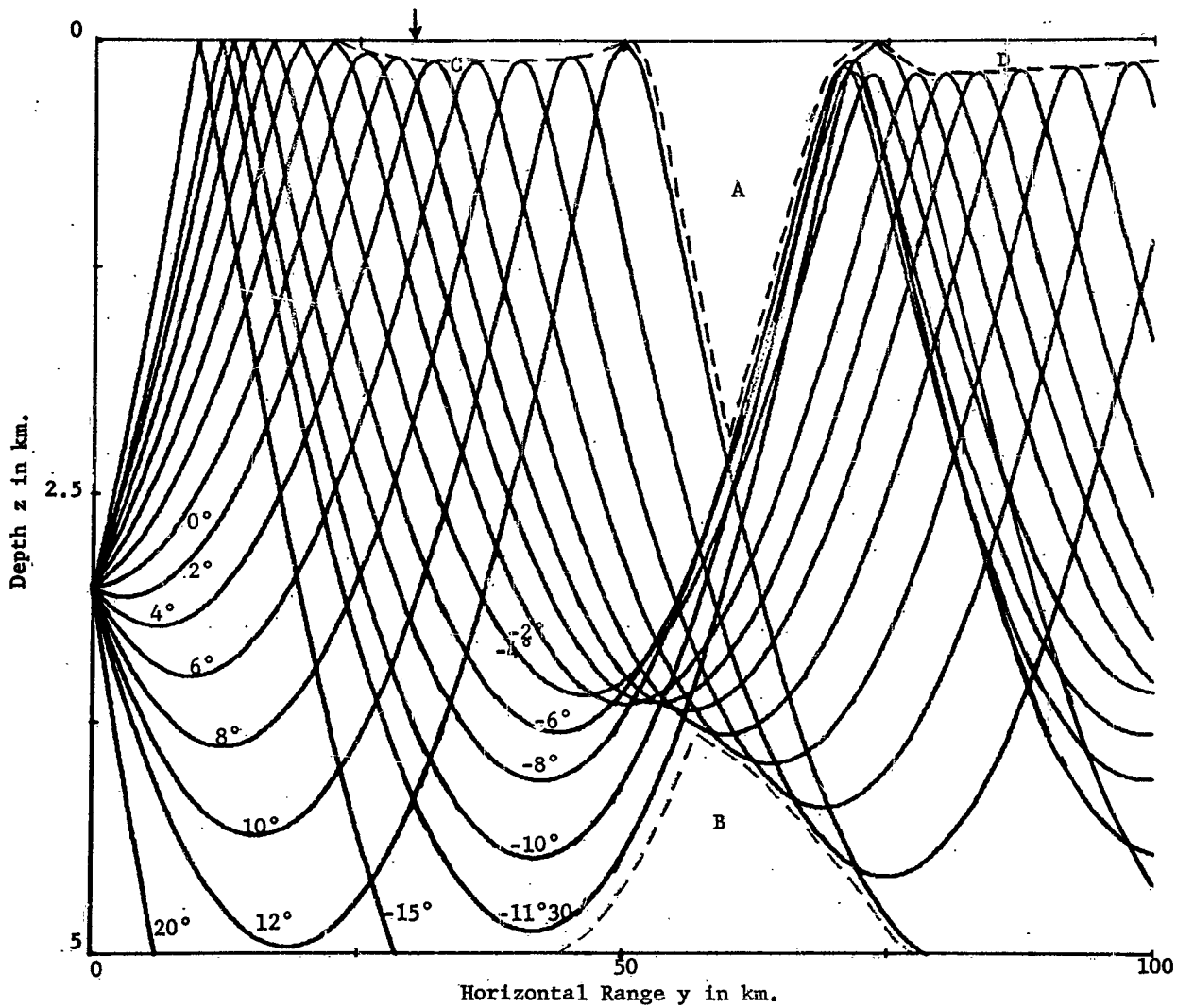

Figure 14: Ray paths in an ocean with a thermal mixing zone. Sound source at z = 3000 m, y = 0 m. (Arrow indicates inflection point of the thermal mixing zone.)

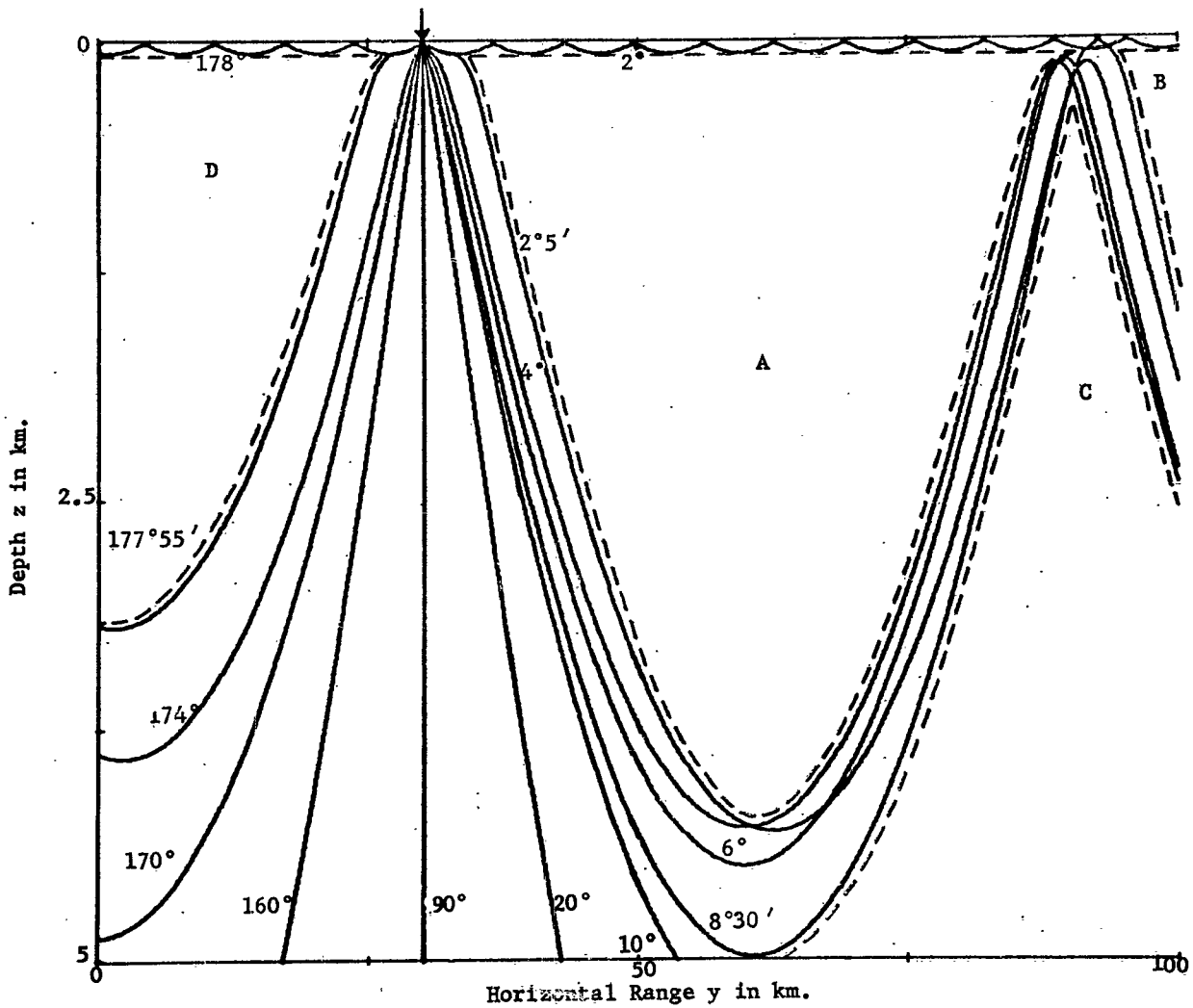

Figure 15: Ray paths in an ocean with a thermal mixing zone. Sound source at z = 0 m, y = 30 km. (Arrow indicates inflection point of the thermal mixing zone.)

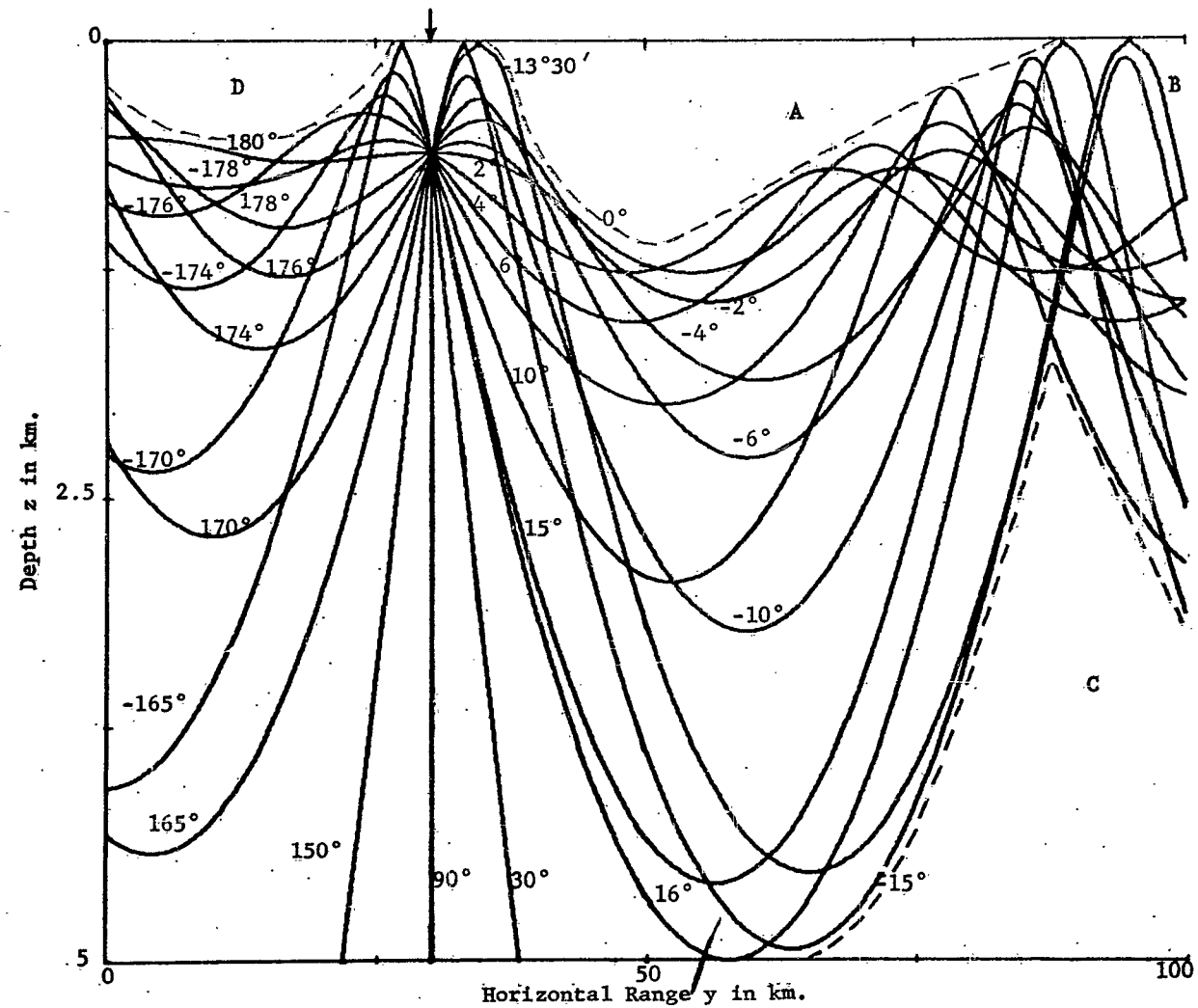

Figure 16: Ray paths in an ocean with a thermal mixing zone. Sound source at z = 600 m, y = 30 km. (Arrow indicates inflection point of the thermal mixing zone.)

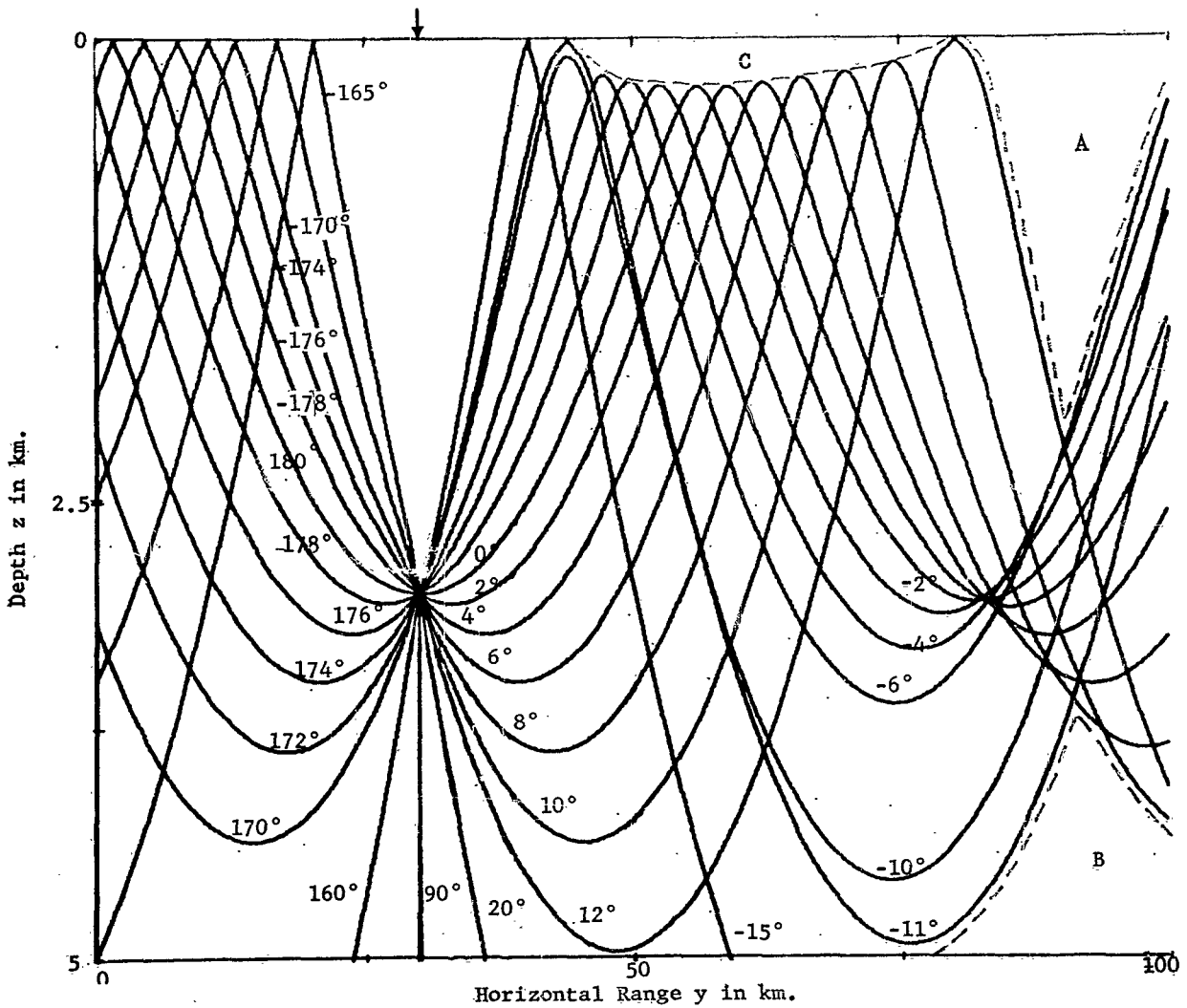

Figure 17: Ray paths in an ocean with a thermal mixing zone. Sound source at z = 3000 m, y = 30 km. (Arrow indicates inflection point of the thermal mixing zone.)

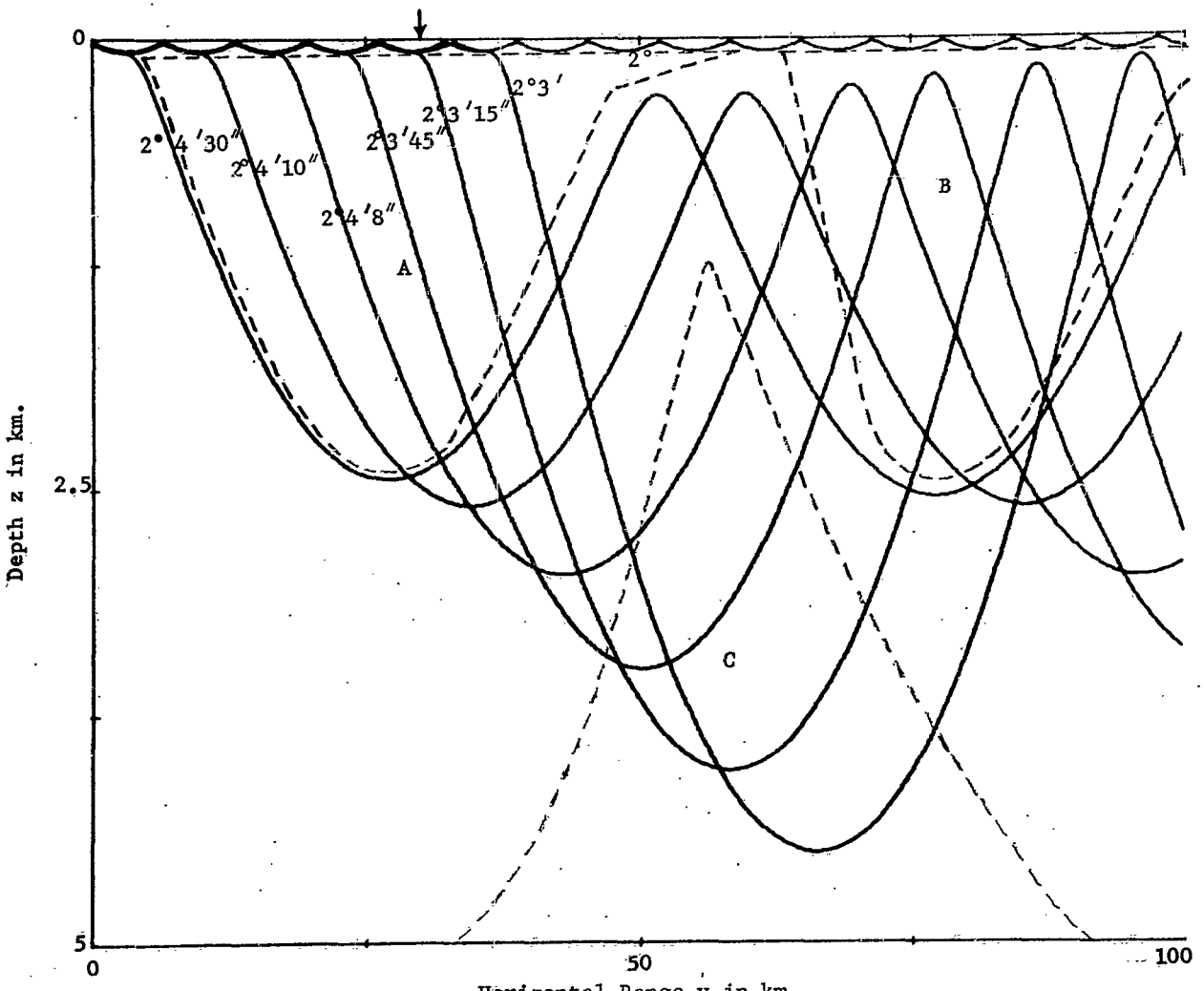

Figure 18: Effect of the thermal mixing zone on shadow zones with the sound source at the surface. Five rays are shown interlacing the shadow zones A, B, and C of Figure 12.

APPENDIX D

DISTRIBUTION

Bureau of Naval Weapons	
DLI-3	1
R-14	1
R-12	1
RREN	1
RRE	1
RT	1
RM	1
Special Projects Office Department of the Navy Washington 25, D. C.	
SP-20	4
SP-43	2
Commander Armed Services Technical Information Agency Arlington Hall Station Arlington 12, Virginia	
Attn: TIPDR	10
Commanding General Aberdeen Proving Ground Aberdeen, Maryland	
Attn: Technical Information Section Development and Proof Services	2
Commander, Operational and Development Force U. S. Atlantic Fleet, U. S. Naval Base Norfolk 11, Virginia	1
Chief of Naval Research Department of the Navy Washington 25, D. C.	
Attn: Code 438	2
Attn: Dr. F. J. Weyl	1
Attn: Fluid Dynamics Branch	1
Director Naval Research Laboratory Washington 25, D. C.	3

DISTRIBUTION (Continued)

Commander Naval Ordnance Laboratory White Oak, Maryland	
Attn: Dr. R. Roberts	1
Attn: Dr. R. E. Wilson	2
Attn: Dr. A. VanTuyl	1
Attn: Technical Library	1
Chief, Bureau of Ships Department of the Navy Washington 25, D. C.	2
Director David Taylor Model Basin Washington 7, D. C.	
Attn: Code 142 (Library Branch)	1
Attn: Code 500 (Technical Director for Hydromechanics Laboratory)	1
Attn: Code 513 (Contract Research Administrator)	1
Attn: Code 520 (Ship Powering Division)	1
Attn: Code 581 (Seaworthiness Fluid Dynamics Division)	1
Attn: Code 820 (Theory Division)	1
Commander U. S. Naval Ordnance Test Station China Lake, California	
Attn: Library	2
Superintendent U. S. Naval Postgraduate School Monterey, California	
Attn: Library, Technical Reports Section	1
Director of the Institute of Naval Studies 185 Alewife Brook Parkway Cambridge 38, Massachusetts	1
Commanding General White Sands Proving Ground La Cruces, New Mexico	
Attn: Flight Determination Laboratory	1

DISTRIBUTION (Continued)

Commander, 3206th Test Group
Building 100
Eglin Air Force Base, Florida
Attn: Mr. H. L. Adams — 1

Commander
Wright Air Development Center
Wright-Patterson Air Force Base
Dayton, Ohio
Attn: WCRRN-4 — 1

U. S. Atomic Energy Commission
Washington, D. C.
Attn: Technical Library — 1

Los Alamos Scientific Laboratory
Los Alamos, New Mexico — 2

Superintendent
U. S. Naval Academy
Annapolis, Maryland
Attn: Library — 1

U. S. Naval Observatory
Washington 25, D. C.
Attn: Dr. G. M. Clemence — 1

U. S. Weather Bureau
Washington 25, D. C.
Attn: Dr. J. Smagorinsky — 1

Commander
Naval Ordnance Test Station
Pasadena Annex
3202 Foothill Boulevard
Pasadena, California — 1

DISTRIBUTION (Continued)

Army Rocket and Guided Missile Agency U. S. Army Ordnance Missile Command Redstone Arsenal, Alabama Attn: Capt. Robert H. C. Au	1
National Aeronautics and Space Administration 1520 H Street, N. W. Washington 25, D. C.	6
Commander Ballistic Missile Division ARDC P. O. Box 262 Inglewood, California Attn: Col. Ebelke (WDTVR)	2
Commanding General Army Ballistic Missile Agency Redstone Arsenal Huntsville, Alabama Attn: Technical Library	1
National Science Foundation 1520 H Street, N. W. Washington, D. C.	
Attn: Engineering Sciences Division	1
Attn: Mathematical Sciences Division	1
Director National Bureau of Standards Washington 25, D. C.	
Attn: Fluid Mechanics Division	1
Attn: Dr. G. B. Schubauer	1
Attn: Dr. G. H. Keulegan	1
Attn: Dr. R. J. Arms	1
Attn: Technical Library	1
Office of Technical Services Department of Commerce Washington, D. C.	1
Guggenheim Aeronautical Laboratory California Institute of Technology Pasadena 4, California	1

DISTRIBUTION (Continued)

University of California
Berkeley 4, California
Attn: Department of Engineering 1

Institute of Mathematical Sciences
New York University
25 Waverly Place
New York 3, New York
Attn: Prof. J. J. Stoker 1
Attn: Prof. B. Haurwitz 1

Harvard University
Cambridge 38, Massachusetts
Attn: Prof. G. Birkhoff 1
Attn: Division of Applied Sciences 1
Attn: Prof. G. F. Carrier 1
Attn: Prof. H. M. Stommel 1

University of Maryland
College Park, Maryland
Attn: Institute for Fluid Dynamics and Applied Mathematics 1

Director
Scripps Institute of Oceanography
University of California
La Jolla, California 1

Massachusetts Institute of Technology
Cambridge, Mass.
Attn: Prof. C. C. Lin 1
Attn: Prof. A. H. Shapiro 1
Attn: Prof. J. G. Charney 1

The Johns Hopkins University
Baltimore 18, Maryland
Attn: Prof. R. R. Long 1

DISTRIBUTION (Continued)

Applied Physics Laboratory
Johns Hopkins University
Silver Spring, Maryland
Attn: Librarian — 2

University of California
San Diego, California
Attn: Prof. W. H. Munk — 1

University of Chicago
Chicago, Illinois
Attn: Prof. H. Riehl — 1

General Electric Co.
Missile and Space Vehicle Department
3198 Chestnut Street
Philadelphia 4, Pennsylvania — 1

Lewis Flight Propulsion Laboratory
National Aeronautics and Space Administration
Cleveland, Ohio — 1

Director
Woods Hole Oceanographic Institution
Woods Hole, Mass. — 2

National Oceanographic Data Center
M and 8th St., S. E.
Washington 25, D. C.
Attn: Librarian — 1

U. S. Navy Oceanographic Office
Washington 25, D. C.
Attn: Librarian — 1

Columbia University
Hudson Laboratories
Dobbs Ferry, N. Y.
Attn: Robert A. Frosch — 1

DISTRIBUTION (Continued)

U. S. Naval Underwater Ordnance Station Newport, Rhode Island	1
Emerson Research Laboratories Silver Spring, Md.	1
Defense Research Laboratories General Motors Corporation Santa Barbara, California	1
Ordnance Research Laboratory The Pennsylvania State University University Park, Pennsylvania	1
Electronic Systems and Products Division The Martin-Marietta Corporation P. O. Box 5837 Orlando, Florida	1
Lockheed Aircraft Corporation Palo Alto, California Attn: Dr. W. C. Griffith	1
Prof. M. Van Dyke Department of Aeronautical Engineering Stanford University Stanford, California	1
Prof. J. Siekmann University of Florida Gainesville, Florida	1
Local:	
D	1
K	1
K-1	1
K-3	1
K-4	1
KXK	1
KXR	1
KXH	1
KYD	2
KYS	1
KXL	50
KXL-1	25
ACL	5
FILE	1

LIBRARY CATALOGING INPUT
PRNC-NWL-5070/15 (7-62)

BIBLIOGRAPHIC INFORMATION

DESCRIPTOR	CODE	DESCRIPTOR	CODE
SOURCE Naval Weapons Laboratory	NPGA	SECURITY CLASSIFICATION AND CODE COUNT UNCLASSIFIED	U021
REPORT NUMBER 1854	1854	CIRCULATION LIMITATION	
REPORT DATE March 1963	0363	CIRCULATION LIMITATION OR BIBLIOGRAPHIC	
		BIBLIOGRAPHIC *(Suppl., Vol., etc.)*	

SUBJECT ANALYSIS OF REPORT

DESCRIPTOR	CODE	DESCRIPTOR	CODE	DESCRIPTOR	CODE
Acoustics	ACOU	Two-dimensional	TWOD		
Rays	RAYS	Effects	EFFE		
Oceans	OCEN	Oceanography	OCEA		
Heat	HEAT	Velocity	VELC		
Source	SOUR	Analysis	ANAL		
Thermal	THER	Computers	COMP		
Mixing	MIXE	Underwater	UNDE		
Zone	ZONE				
Eikonal (Mathematics)	EIKO				
Differential	DIFE				
Equations	EQUA				
Mathematics	MATH				
Refraction	REFC				
Refractive index	REFT				

Naval Weapons Laboratory, Dahlgren, Virginia.
(NWL Report No. 1854)
ACOUSTIC RAYS IN AN OCEAN WITH HEAT SOURCE OR THERMAL MIXING ZONE, by H. J. Lugt and Peter Ugincius. Mar 1963.
17 p., 18 figs., 1 table.

UNCLASSIFIED

The eikonal equation of ray acoustics is discussed for the general case, with the index of refraction a function of the three space coordinates. Two examples illustrating the influences of a two-dimensional heat source and a thermal mixing zone on the acoustic ray paths are presented. Numerical results show that for long range acoustical ray tracing inhomogeneities of the ocean in the horizontal plane can cause refraction effects, which are not negligible in comparison with effects in the vertical direction.

1. Acoustic rays
2. Oceanography
3. Water - Refractive index
4. Differential equations
I. Lugt, H. J.
II. Ugincius, P.

Task: R360FR103/2101/R01101001

UNCLASSIFIED

Naval Weapons Laboratory, Dahlgren, Virginia.
(NWL Report No. 1854)
ACOUSTIC RAYS IN AN OCEAN WITH HEAT SOURCE OR THERMAL MIXING ZONE, by H. J. Lugt and Peter Ugincius. Mar 1963.
17 p., 18 figs., 1 table.

UNCLASSIFIED

The eikonal equation of ray acoustics is discussed for the general case, with the index of refraction a function of the three space coordinates. Two examples illustrating the influences of a two-dimensional heat source and a thermal mixing zone on the acoustic ray paths are presented. Numerical results show that for long range acoustical ray tracing inhomogeneities of the ocean in the horizontal plane can cause refraction effects, which are not negligible in comparison with effects in the vertical direction.

1. Acoustic rays
2. Oceanography
3. Water - Refractive index
4. Differential equations
I. Lugt, H. J.
II. Ugincius, P.

Task: R360FR103/2101/R01101001

UNCLASSIFIED

Naval Weapons Laboratory, Dahlgren, Virginia.
(NWL Report No. 1854)
ACOUSTIC RAYS IN AN OCEAN WITH HEAT SOURCE OR THERMAL MIXING ZONE, by H. J. Lugt and Peter Ugincius. Mar 1963.
17 p., 18 figs., 1 table.

UNCLASSIFIED

The eikonal equation of ray acoustics is discussed for the general case, with the index of refraction a function of the three space coordinates. Two examples illustrating the influences of a two-dimensional heat source and a thermal mixing zone on the acoustic ray paths are presented. Numerical results show that for long range acoustical ray tracing inhomogeneities of the ocean in the horizontal plane can cause refraction effects, which are not negligible in comparison with effects in the vertical direction.

1. Acoustic rays
2. Oceanography
3. Water - Refractive index
4. Differential equations
I. Lugt, H. J.
II. Ugincius, P.

Task: R360FR103/2101/R01101001

UNCLASSIFIED

Naval Weapons Laboratory, Dahlgren, Virginia.
(NWL Report No. 1854)
ACOUSTIC RAYS IN AN OCEAN WITH HEAT SOURCE OR THERMAL MIXING ZONE, by H. J. Lugt and Peter Ugincius. Mar 1963.
17 p., 18 figs., 1 table.

UNCLASSIFIED

The eikonal equation of ray acoustics is discussed for the general case, with the index of refraction a function of the three space coordinates. Two examples illustrating the influences of a two-dimensional heat source and thermal mixing zone on the acoustic ray paths are presented. Numerical results show that for long range acoustical ray tracing inhomogeneities of the ocean in the horizontal plane can cause refraction effects, which are not negligible in comparison with effects in the vertical direction.

1. Acoustic rays
2. Oceanography
3. Water - Refractive index
4. Differential equations
I. Lugt, H. J.
II. Ugincius, P.

Task: R360FR103/2101/R01101001

UNCLASSIFIED